Critical Behavior and Universal Signature of an Axion Insulator State

Hailong Li,[1] Hua Jiang,[2,3] Chui-Zhen Chen,[2,3,*] and X. C. Xie[1,4,5,†]
[1]*International Center for Quantum Materials, School of Physics, Peking University, Beijing 100871, China*
[2]*School of Physical Science and Technology, Soochow University, Suzhou 215006, China*
[3]*Institute for Advanced Study, Soochow University, Suzhou 215006, China*
[4]*Beijing Academy of Quantum Information Sciences, Beijing 100193, China*
[5]*CAS Center for Excellence in Topological Quantum Computation, University of Chinese Academy of Sciences, Beijing 100190, China*

(Received 6 November 2020; accepted 12 March 2021; published 12 April 2021)

Recently, the search for an axion insulator state in the ferromagnetic-3D topological insulator (TI) heterostructure and $MnBi_2Te_4$ has attracted intense interest. However, its detection remains difficult in experiments. We systematically investigate the disorder-induced phase transition of the axion insulator state in a 3D TI with antiparallel magnetization alignment surfaces. It is found that there exists a 2D disorder-induced phase transition on the surfaces of the 3D TI which shares the same universality class with the quantum Hall plateau to plateau transition. Then, we provide a phenomenological theory which maps the random mass Dirac Hamiltonian of the axion insulator state into the Chalker-Coddington network model. Therefore, we propose probing the axion insulator state by investigating the universal signature of such a phase transition in the ferromagnetic-3D TI heterostructure and $MnBi_2Te_4$. Our findings not only show a global phase diagram of the axion insulator state, but also stimulate further experiments to probe it.

DOI: 10.1103/PhysRevLett.126.156601

Introduction.—Topology and symmetry breaking play a key role in describing phases of matter. Since proposed in 2008, the axion insulator state has attracted extensive experimental and theoretical studies [1–8]. The 3D topological insulator (TI) is a time-reversal symmetry-protected topological matter characterized by gapless Dirac surface states in the bulk gap [1]. If the time-reversal symmetry is broken, an axion insulator state shows up when the gapless Dirac surface states are gapped out by the magnetizations pointing outward from (inward to) the surfaces [1,2]. In comparison with a trivial insulator state, the axion insulator state possesses a unique electromagnetic response from the massive Dirac surface states, giving rise to novel phenomena such as a quantized topological magnetoelectric effect and half-quantized surface Hall conductance [2–5]. In the experiment, the axion insulator shows huge longitudinal resistance and zero Hall conductance, because the top and bottom surface Hall conductance cancels out [7–9]. These results, however, coincide with a trivial band insulator. Therefore, definitive experimental evidence for the axion insulator state is still missing.

On the other hand, typical properties of Anderson phase transitions in disordered systems, especially the critical exponents, depend only on general properties of the model, such as spatial dimensionality, symmetry, etc. The experimental studies of the quantum phase transition have already been extensively performed in magnetic TIs and revealed unique properties of topological states [9–16]. In this work, we propose probing the axion insulator state by shedding light on the disorder-induced metal-insulator transition in 3D magnetic TIs. We systematically study the disorder

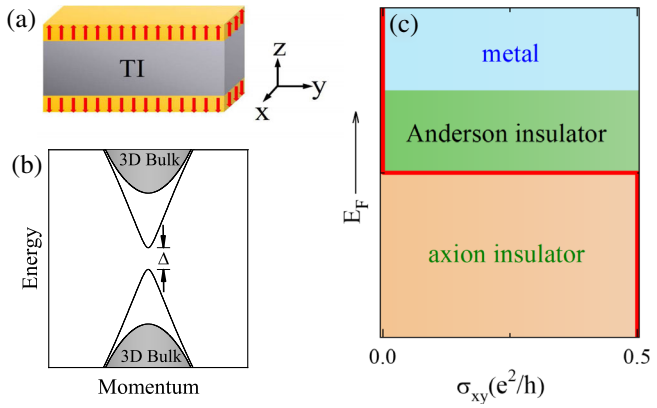

FIG. 1. (a) Schematic plot of an axion insulator consisting of a 3D time-reversal invariant TI with antiparallel magnetization alignment surfaces. (b) The magnetization term can open a gap Δ at the Dirac point of the surface states. (c) Schematic phase diagram of the 3D TI with antiparallel magnetization alignment surfaces under weak disorder. The red curve depicts the Hall conductance varying with the Fermi energy. Given the difficulty in detecting the quantized surface Hall conductance, the phase transition between the axion insulator and the Anderson insulator is proposed as a universal experimental signature of an axion insulator.

effect of a 3D TI with antiparallel magnetization alignment surfaces and give a global phase diagram. Notably, there exists a 2D quantum-Hall-type phase transition between the axion insulating phase and the Anderson insulating phase, which provides a universal experimental signature of an axion insulator state [see Fig. 1(c)]. Specifically, with the weak disorder and increase in the Fermi energy, the axion insulator will undergo a 2D delocalized transition on the surfaces of the 3D TI, become an Anderson insulator, and then transform into a diffusive metal after a 3D insulator-metal transition. We also provide a phenomenological theory that relates the disordered axion insulator to the Chalker-Coddington network model. Furthermore, the 2D phase transition remains in the presence of bulk antiferromagnetism for $MnBi_2Te_4$, and thereby, it is model independent. The universal phase transition behavior of the axion insulator we predicted can be detected in the ferromagnetic-3D TI heterostructure and the antiferromagnetic TI $MnBi_2Te_4$ [9,15–22].

Effective model of the axion insulators.—We consider a 3D TI with antiparallel magnetization alignment surfaces [see Fig. 1(a)] that has been realized in experiments [6,7,9], and the four-band effective Hamiltonian is

$$H = H_0 + H_M, \tag{1}$$

where $H_0(\mathbf{k}) = \sum_{i=1}^{4} d_i(\mathbf{k})\Gamma_i$ with $d_1 = A_1 k_x$, $d_2 = A_1 k_y$, $d_3 = A_2 k_z$, and $d_4 = M_0 - B_1 k_z^2 - B_2(k_x^2 + k_y^2)$. It describes a time-reversal invariant TI and hosts a single Dirac cone on each surface [1]. Here, A_i and B_i are model parameters, and M_0 controls the bulk gap of the 3D TI. $\Gamma_i = s_i \otimes \sigma_1$ for $i = 1, 2, 3$, and $\Gamma_4 = s_0 \otimes \sigma_3$. s_i and σ_i are the Pauli matrices for the spin and orbital degrees of freedom. The Zeeman splitting $H_M = M(z)s_z \otimes \sigma_0$ where $M(z)$ takes the values $\pm M_z$ on the top and bottom surfaces, respectively, and zero elsewhere [see Fig. 1(a)]. Such a time-reversal breaking mass term will open up a Dirac gap $\Delta \approx 2|M_z|$ on the top or bottom surface [see Fig. 1(b)], which is described by $H_{\mathrm{surf}}^{t/p} = A_1(\sigma_x k_x + \sigma_x k_x) \pm M_z\sigma_z$ and leads to a half-quantized Hall conductance $\sigma_{xy}^{t/b} = \pm(e^2/2h)$ for the top or bottom surface [2]. Note that we have demonstrated the existence of an axion insulating phase by numerically calculating half-quantized surface Hall conductance and discretizing Hamiltonian H on square lattices [23].

Unlike the quantum anomalous Hall insulator, the total Hall conductance of the axion insulator is zero, i.e., $\sigma_{xy}^t + \sigma_{xy}^b = 0$, and there are no chiral edge modes within the surface gap. This explains why a zero Hall conductance plateau and a huge longitudinal resistance were observed for the axion insulator state in the recent experiments [7–9]. However, these results are coincident with a trivial band insulator. To unveil signatures of the axion insulator, we will investigate the disorder-induced critical behavior of the axion insulator in the following. We include the random magnetic disorder as $H_D = V(\mathbf{r})s_z \otimes \sigma_0$ where $V(\mathbf{r})$ is uniformly distributed within $[-W/2, W/2]$ with W denoting the disorder strength.

Quantum-Hall-type phase transition.—To calculate the localization length, we consider a 3D long bar sample of length L_y and widths $L_x = L_z = L$ with the periodic boundary condition in the x direction and open boundary conditions in the y and z directions unless otherwise specified. The localization length $\lambda(L)$ is obtained by transfer matrix method [24–26]. Generally, criticality can be accessed from the renormalized localization length $\Lambda = \lambda/L$, which increases with L in a metallic phase, decreases with L in an insulating phase, and does not depend on L at the critical point.

We consider a sample like Fig. 1(a) and perform a finite-size scaling analysis as shown in Fig. 2. It shows that the axion insulator undergoes multiple phase transitions with increasing Fermi energy E_F under

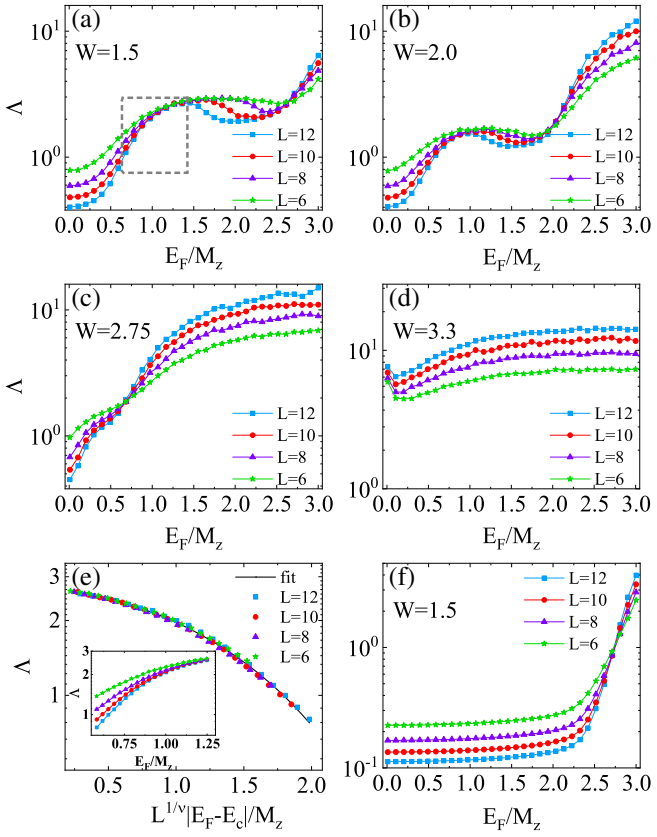

FIG. 2. (a)–(d) Renormalized localization length $\Lambda = \lambda(L)/L$ against the Fermi energy E_F at different magnetic disorder strengths W. The curves correspond to different sample widths L. (e) Shows a fit of the numerical data in the inset with $W = 1.5$ by a scaling function $\Lambda = f(L^{1/\nu}|E_F - E_c|/M_z)$. The polynomial fitting method gives a critical exponent $\nu = 2.654 \pm 0.213$ and a critical Fermi energy $E_c = 0.164 \pm 0.005$. Here, the raw data is obtained from the grey rectangle region of (a). (f) Λ with periodic boundary conditions in the x and z directions and $W = 1.5$. Other parameters are fixed as $A_1 = A_2 = 0.55$, $B_1 = B_2 = 0.25$, $M_0 = 0.3$, and $M_z = 0.12$.

different disorder strengths W. Specifically, for weak disorder $W = 1.5$ and 2 in Figs. 2(a) and 2(b), one can identify an axion insulator phase with $d\Lambda/dL < 0$ when $|E_F/M_z| \lesssim 1$, where the Fermi energy E_F is within the surface Dirac gap M_z. With increasing Fermi energy, the system goes delocalized with $d\Lambda/dL = 0$ and arrives at an Anderson insulator phase without half-quantized Hall conductance as we will show below. This is reminiscent of the plateau-plateau transition in the 2D quantum Hall system. To identify that such a phase transition belongs to the quantum Hall type, we perform a single-parameter scaling analysis in Fig. 2(e) [27]. The critical exponent ν which is expected to exhibit universality is extracted as 2.654 ± 0.213. This estimate of ν is in agreement with recent numerical results, $\nu \sim 2.6$, based on the Chalker-Coddington model of the integer quantum Hall effect [28–30]. Note that, as long as the magnetic disorder dominates over the Anderson disorder, the existence of the 2D quantum-Hall-type transition remains [23]. Moreover, to verify that the phase transition comes from two-dimensional Dirac surfaces, we take periodic boundary conditions in both x and z directions and calculate Λ in Fig. 2(f). In comparison to Fig. 2(a), one can see the lower 2D delocalized state disappears, and only the higher critical point remains, which indicates a 3D Anderson metal-insulator transition. As a result, there exists a universal 2D quantum-Hall-type phase transition on the surfaces of the axion insulator which, thus, provides a universal signature of the axion insulator state in experiment [23]. Here, the localization length exponent $\nu = p/2\kappa$ is determined directly from the measured κ and p, and they can be directly obtained from the transport measurement experimentally [31]. Finally, in the large disorder limit, the axion insulator is gradually suppressed by the 3D critical point, and eventually disappears [see Figs. 2(a)–2(d)], and the system becomes a 3D diffusive metal. This can be seen more easily in the phase diagram [see Fig. 3(d)].

Hall conductance and phase diagram.—Next, we investigate the Hall conductance to further identify the two insulating phases illustrated above. For a low Fermi energy and if the system is in an axion insulating state, the surface Hall conductance and the net Hall conductance of the whole sample are expected to be half-quantized and zero, respectively. On the other hand, when the Fermi energy goes across the 2D delocalized state, the system is converted into an Anderson insulator and the surface Hall conductance is expected to lose its half-integer quantization and approach zero. Note that, in realistic materials such as ferromagnetic-TI heterostructures and antiferromagnetic TI $MnBi_2Te_4$, the magnetizations are pointing in the z direction, and thereby, the phase transition occurs only on the top and bottom surface.

Here, the layer-dependent Hall conductance is evaluated by a real-space Kubo formula [32,33],

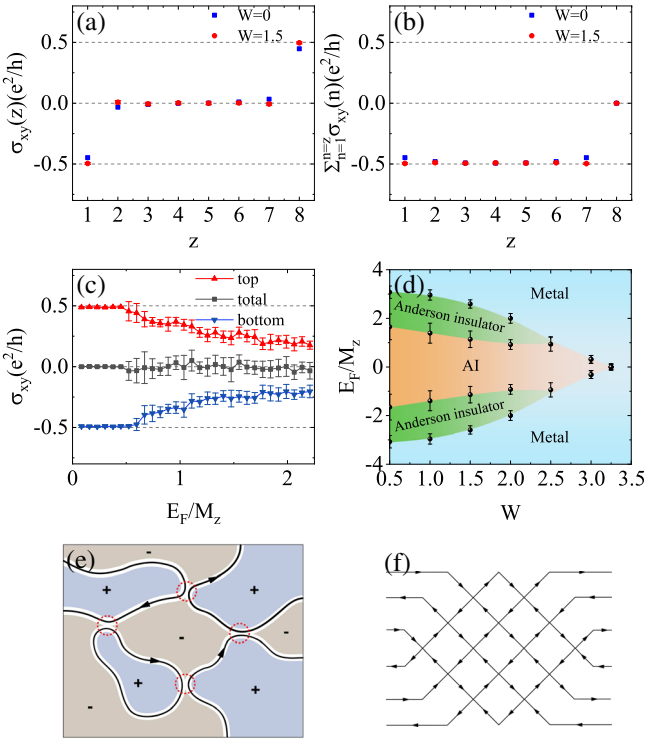

FIG. 3. (a) The Hall conductance as a function of the layer index z with $z = 1$ for the bottom layer and $z = 8$ for the top layer. (b) The cumulative summation of the Hall conductance from $z = 1$ to the zth layer is disorder averaged. (c) The Hall conductance of the top surface states $[\sum_{n=7}^{n=8}\sigma_{xy}(n)]$, the bottom surface states $[\sum_{n=1}^{n=2}\sigma_{xy}(n)]$ and the whole sample $[\sum_{n=1}^{n=8}\sigma_{xy}(n)]$. (d) Phase diagram of a disordered axion insulator (AI) in the $E_F/M_z - W$ plane. (e) Chiral edge states along domain walls of Dirac fermions with positive (+) and negative (−) masses. (f) The Chalker-Coddington network model on a quasi-1D system, where a scattering matrix describes the scattering from two incoming to two outgoing modes at each node (crossing point).

$$\sigma_{xy}(z) = \frac{2\pi i e^2}{h}\langle \mathrm{Tr}\{P[-i[\hat{x}, P], -i[\hat{y}, P]]\}_z\rangle_W, \quad (2)$$

with periodic boundary conditions in both x and y directions. $\langle\ldots\rangle_W$ represents the disorder average, $(\hat{x}, \hat{y})$ denotes the position operator, and $\mathrm{Tr}\{\ldots\}_z$ is trace over the wave functions of the zth layer. P is the projector onto the occupied states of H. Through Eq. (2), we calculate the layer-dependent Hall conductance $\sigma_{xy}(z)$ [see Fig. 3(a)]. For both a clean sample ($W = 0$) and a disordered sample ($W = 1.5$), the nonzero Hall conductance mainly comes from surfaces near the top ($z = 1$) and bottom ($z = 8$) layers, while it decays exponentially into bulk (between $z = 2$ and $z = 7$). This is coincident with the exponential decay of the surface states in 3D TI, where the surface states exist in several layers near the surfaces [34]. To gain further insight into the Hall

conductance, we take the total Hall conductance of the several layers into consideration. The cumulative summation of the contribution from each layer, i.e., $\sum_{n=1}^{n=z}\sigma_{xy}(n)$, is shown in Fig. 3(b). For $W=1.5$ ($W=0$), the cumulative Hall conductance becomes half-quantized at $z=1$ ($z=2$) indicating that the bottom surface Hall conductance is half-quantized. Besides, when $z=8$, the net Hall conductance of the whole sample vanishes for both cases since the half-quantized Hall conductance of the top and bottom surfaces cancel each other out. Moreover, in Fig. 3(c), one can see a half-quantized surface Hall conductance plateau for the axion insulator at the lower energy regime ($|E_F/M_z| \lesssim 0.5$), while it gradually approaches zero for the Anderson insulator at the high energy regime.

Now, we perform finite-size scaling analysis under various disorder strengths and summarize a phase diagram in the $E_F/M_z - W$ plane [see Fig. 3(d)]. Because of the particle-hole symmetry of the Hamiltonian H, the phase diagram is symmetric about $E_F/M_z=0$. For weak W, the axion insulator and the 3D diffusive metal phases are separated by the Anderson insulator phase. With the increase of the disorder strength, they gradually draw close to each other and are connected, eventually, at a large disorder strength $W\approx 2.5$. Then, the bulk gap continues to shrink and close at about $W\approx 3.2$, and the sample ends up as a 3D metal [35], which manifests the features of levitation and pair annihilation [36].

To understand the underlying mechanism for the above 2D phase transition, we provide a phenomenological explanation. When $W=0$, the surface state satisfies a 2D Dirac Hamiltonian with a spatially homogenous mass. With the increase of the random magnetic (mass) disorder W, the surface mass becomes spatially inhomogeneous such that the Dirac fermions with positive and negative masses coexist. In this case, the system can be described by a 2D random Dirac mass Hamiltonian as long as the Fermi energy is much smaller than the 3D mobility edge where the bulk states can be safely ignored. In Fig. 3(e), a chiral edge state exists between two regions with Dirac masses of opposite signs [37]. Moreover, the 2D random Dirac mass Hamiltonian can be mapped onto the Chalker-Coddington model which describes the quantum Hall plateau to plateau transition [37–39]. Figure 3(f) shows the Chalker-Coddington network model on a quasi-1D system. At each node, the incoming and outgoing channels denote the chiral edge modes confined at domain walls between Dirac fermions of opposite signs in Fig. 3(e). Thus, the Chalker-Coddington model is equivalent to the random Dirac Hamiltonian [37–39]. Moreover, the critical exponent $\nu=2.654\pm0.213$ in our model agrees with previous numerical results $\nu\sim 2.6$, based on the Chalker-Coddington model [28–30]. Consequently, the phase transition from the axion insulator to the Anderson insulator shares the same universality class with the quantum Hall transition.

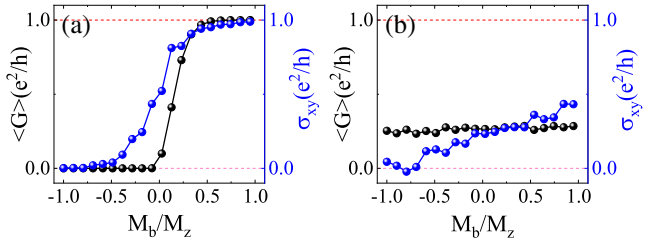

FIG. 4. Disorder-averaged conductance $\langle G\rangle$ and total Hall conductance σ_{xy} as functions of the magnetization in the bottom surface M_b. (a) The axion insulating phase with $E_F/M_z\approx 0.083$. (b) The Anderson insulating phase with $E_F/M_z=2$. Other parameters: the disorder strength $W=1.5$ and the system size $L_z\times L_x\times L_y=8\times 40\times 400$.

Discussions and experimental routines.—Recently, the axion insulator state was reported experimentally in the ferromagnetic-3D TI heterostructure and the antiferromagnetic TI $MnBi_2Te_4$ [7–9,14]. They found a phase transition from an axion insulator state to a Chern insulator state as the Hall conductance increased from zero to e^2/h, when the magnetizations of the top and bottom surfaces were driven from an antiparallel alignment to a parallel alignment by sweeping an external magnetic field [9,14]. However, these results coincide with the trivial band insulator in magnetic TI systems [11,12]. In Fig. 4(a), if we start with the axion insulator phase for antiparallel alignment configuration ($M_zM_b<0$), both the two-terminal conductance [40–42] and the Hall conductance increase from zero to e^2/h by the magnetic flipping of the bottom surface. This demonstrates the axion insulator to Chern insulator transition as observed in experiments. On the contrary, for the Anderson insulator, the two-terminal conductance keeps small and the Hall conductance does not show any quantized behavior [see Fig. 4(b)]. Thus, we conclude that these reported experimental systems are probably in the axion insulating phase but cannot be in the Anderson insulating phase. They are good candidate materials to further identify the axion insulator by probing the universal 2D phase transition, thereby ruling out the trivial band insulator.

Regarding the difficulty in varying the Fermi energy in a 3D sample, we suggest applying an in-plane magnetic field in the x (y) direction. It will increase E_F/M_z by reducing the out-of-plane magnetization M_z, and the 2D phase transition can appear [43]. Moreover, we further include the bulk antiferromagnetism of the Hamiltonian H in Eq. (1) as an effective model of $MnBi_2Te_4$ [21,44,45] and repeat the finite-size scaling [23]. The 2D phase transition remains and, thereby, is model independent [23]. Therefore, we propose probing the universal 2D phase transition of the axion insulator in a ferromagnetic-3D TI heterostructure or an antiferromagnetic TI $MnBi_2Te_4$.

Conclusion.—To summarize, we investigate the disorder-induced Anderson transition of an axion insulator and find a 2D phase transition between the axion insulating phase and

the Anderson insulating phase, which does not occur in trivial band insulators. The 2D phase transition originates from the 2D massive Dirac Hamiltonian which lives on the surfaces of a 3D system. From the viewpoint of the Chalker-Coddington network model, an exponent $\nu \approx 2.65$ strongly suggests the 2D phase transition shares the same universality class with the quantum Hall plateau to plateau transition. Therefore, we propose probing the axion insulator state by investigating the universal signature of 2D quantum-Hall-type critical behaviors in 3D magnetic TIs.

This work is financially supported by the National Basic Research Program of China (Grants No. 2019YFA0308403, and No. 2015CB921102), the National Natural Science Foundation of China (Grants No. 11974256, and No. 11822407), the Strategic Priority Research Program of the Chinese Academy of Sciences (Grant No. XDB28000000), and funded by the Priority Academic Program Development (PAPD) of Jiangsu Higher Education Institutions. C.-Z. C. is also funded by the Natural Science Foundation of Jiangsu Province Grant No. BK20190813.

Note added.—Recently, we became aware of an independent study [46] which focuses on similar topics but different aspects.

*czchen@suda.edu.cn
†xcxie@pku.edu.cn

[1] X.-L. Qi and S.-C. Zhang, Topological insulators and superconductors, Rev. Mod. Phys. **83**, 1057 (2011).
[2] X.-L. Qi, T. L. Hughes, and S.-C. Zhang, Topological field theory of time-reversal invariant insulators, Phys. Rev. B **78**, 195424 (2008).
[3] T. Morimoto, A. Furusaki, and N. Nagaosa, Topological magnetoelectric effects in thin films of topological insulators, Phys. Rev. B **92**, 085113 (2015).
[4] J. Yu, J. Zang, and C.-X. Liu, Magnetic resonance induced pseudoelectric field and giant current response in axion insulators, Phys. Rev. B **100**, 075303 (2019).
[5] K. Nomura and N. Nagaosa, Surface-Quantized Anomalous Hall Current and the Magnetoelectric Effect in Magnetically Disordered Topological Insulators, Phys. Rev. Lett. **106**, 166802 (2011).
[6] J. Wang, B. Lian, X.-L. Qi, and S.-C. Zhang, Quantized topological magnetoelectric effect of the zero-plateau quantum anomalous hall state, Phys. Rev. B **92**, 081107(R) (2015).
[7] D. Xiao, J. Jiang, J.-H. Shin, W. Wang, F. Wang, Y.-F. Zhao, C. Liu, W. Wu, M. H. W. Chan, N. Samarth, and C.-Z. Chang, Realization of the Axion Insulator State in Quantum Anomalous Hall Sandwich Heterostructures, Phys. Rev. Lett. **120**, 056801 (2018).
[8] M. Mogi, M. Kawamura, R. Yoshimi, A. Tsukazaki, Y. Kozuka, N. Shirakawa, K. S. Takahashi, M. Kawasaki, and Y. Tokura, A magnetic heterostructure of topological insulators as a candidate for an axion insulator, Nat. Mater. **16**, 516 (2017).
[9] C. Liu, Y. Wang, H. Li, Y. Wu, Y. Li, J. Li, K. He, Y. Xu, J. Zhang, and Y. Wang, Robust axion insulator and Chern insulator phases in a two-dimensional antiferromagnetic topological insulator, Nat. Mater. **19**, 522 (2020).
[10] J. Checkelsky, R. Yoshimi, A. Tsukazaki, K. Takahashi, Y. Kozuka, J. Falson, M. Kawasaki, and Y. Tokura, Trajectory of the anomalous Hall effect towards the quantized state in a ferromagnetic topological insulator, Nat. Phys. **10**, 731 (2014).
[11] X. Kou, L. Pan, J. Wang, Y. Fan, E. S. Choi, W.-L. Lee, T. Nie, K. Murata, Q. Shao, S.-C. Zhang *et al.*, Metal-to-insulator switching in quantum anomalous Hall states, Nat. Commun. **6**, 8474 (2015).
[12] Y. Feng, X. Feng, Y. Ou, J. Wang, C. Liu, L. Zhang, D. Zhao, G. Jiang, S.-C. Zhang, K. He, X. Ma, Q.-K. Xue, and Y. Wang, Observation of the Zero Hall Plateau in a Quantum Anomalous Hall Insulator, Phys. Rev. Lett. **115**, 126801 (2015).
[13] C.-Z. Chang, W. Zhao, J. Li, J. K. Jain, C. Liu, J. S. Moodera, and M. H. W. Chan, Observation of the Quantum Anomalous Hall Insulator to Anderson Insulator Quantum Phase Transition and Its Scaling Behavior, Phys. Rev. Lett. **117**, 126802 (2016).
[14] X. Wu, D. Xiao, C.-Z. Chen, J. Sun, L. Zhang, M. H. W. Chan, N. Samarth, X. C. Xie, X. Lin, and C.-Z. Chang, Scaling behavior of the quantum phase transition from a quantum-anomalous-Hall insulator to an axion insulator, Nat. Commun. **11**, 4532 (2020).
[15] J. Ge, Y. Liu, J. Li, H. Li, T. Luo, Y. Wu, Y. Xu, and J. Wang, High-Chern-number and high-temperature quantum Hall effect without Landau levels, Natl. Sci. Rev. **7**, 1280 (2020).
[16] Y. Deng, Y. Yu, M. Z. Shi, Z. Guo, Z. Xu, J. Wang, X. H. Chen, and Y. Zhang, Quantum anomalous Hall effect in intrinsic magnetic topological insulator $MnBi_2Te_4$, Science **367**, 895 (2020).
[17] Y. Gong *et al.*, Experimental realization of an intrinsic magnetic topological insulator, Chin. Phys. Lett. **36**, 076801 (2019).
[18] J. Zhang, Z. Liu, and J. Wang, In-plane magnetic-field-induced quantum anomalous Hall plateau transition, Phys. Rev. B **100**, 165117 (2019).
[19] J. Li, Y. Li, S. Du, Z. Wang, B.-L. Gu, S.-C. Zhang, K. He, W. Duan, and Y. Xu, Intrinsic magnetic topological insulators in van der Waals layered $MnBi_2Te_4$—family materials, Sci. Adv. **5**, eaaw5685 (2019).
[20] M. M. Otrokov *et al.*, Prediction and observation of an antiferromagnetic topological insulator, Nature (London) **576**, 416 (2019).
[21] R.-X. Zhang, F. Wu, and S. Das Sarma, Möbius Insulator and Higher-Order Topology in $MnBi_{2n}Te_{3n+1}$, Phys. Rev. Lett. **124**, 136407 (2020).
[22] Y.-J. Hao *et al.*, Gapless Surface Dirac Cone in Antiferromagnetic Topological Insulator $MnBi_2Te_4$, Phys. Rev. X **9**, 041038 (2019).
[23] See Supplemental Material at http://link.aps.org/supplemental/10.1103/PhysRevLett.126.156601 for detailed discussions.
[24] B. Kramer and A. MacKinnon, Localization: Theory and experiment, Rep. Prog. Phys. **56**, 1469 (1993).
[25] A. MacKinnon and B. Kramer, One-Parameter Scaling of Localization Length and Conductance in Disordered Systems, Phys. Rev. Lett. **47**, 1546 (1981).

[26] A. MacKinnon and B. Kramer, The scaling theory of electrons in disordered solids: Additional numerical results, Z. Phys. B **53**, 1 (1983).
[27] H. Obuse, A. Furusaki, S. Ryu, and C. Mudry, Two-dimensional spin-filtered chiral network model for the F_2 quantum spin-Hall effect, Phys. Rev. B **76**, 075301 (2007).
[28] M. Amado, A. V. Malyshev, A. Sedrakyan, and F. Dominguez-Adame, Numerical Study of the Localization Length Critical Index in a Network Model of Plateau-Plateau Transitions in the Quantum Hall Effect, Phys. Rev. Lett. **107**, 066402 (2011).
[29] H. Obuse, I. A. Gruzberg, and F. Evers, Finite-Size Effects and Irrelevant Corrections to Scaling Near the Integer Quantum Hall Transition, Phys. Rev. Lett. **109**, 206804 (2012).
[30] K. Slevin and T. Ohtsuki, Critical exponent for the quantum Hall transition, Phys. Rev. B **80**, 041304(R) (2009).
[31] W. Li, C. L. Vicente, J. S. Xia, W. Pan, D. C. Tsui, L. N. Pfeiffer, and K. W. West, Scaling in Plateau-to-Plateau Transition: A Direct Connection of Quantum Hall Systems with the Anderson Localization Model, Phys. Rev. Lett. **102**, 216801 (2009).
[32] E. Prodan, Robustness of the spin-Chern number, Phys. Rev. B **80**, 125327 (2009).
[33] E. Prodan, Disordered topological insulators: Aa non-commutative geometry perspective, J. Phys. A **44**, 239601 (2011).
[34] W.-Y. Shan, H.-Z. Lu, and S.-Q. Shen, Effective continuous model for surface states and thin films of three-dimensional topological insulators, New J. Phys. **12**, 043048 (2010).
[35] If a system is topological nontrivial in the clean limit, the system has to close the bulk gap with increasing disorder, so that it can finally turn into an Anderson insulator in the large disorder limit.
[36] M. Onoda, Y. Avishai, and N. Nagaosa, Localization in a Quantum Spin Hall System, Phys. Rev. Lett. **98**, 076802 (2007).
[37] A. W. W. Ludwig, M. P. A. Fisher, R. Shankar, and G. Grinstein, Integer quantum Hall transition: An alternative approach and exact results, Phys. Rev. B **50**, 7526 (1994).
[38] J. T. Chalker and P. D. Coddington, Percolation, quantum tunnelling and the integer Hall effect, J. Phys. C **21**, 2665 (1988).
[39] C. M. Ho and J. T. Chalker, Models for the integer quantum Hall effect: The network model, the dirac equation, and a tight-binding hamiltonian, Phys. Rev. B **54**, 8708 (1996).
[40] A. MacKinnon, The calculation of transport properties and density of states of disordered solids, Z. Phys. B **59**, 385 (1985).
[41] A. MacKinnon, L. Schweitzer, and B. Kramer, Magneto-transport in two dimensions: Some numerical results, Surf. Sci. **142**, 189 (1984).
[42] L. Schweitzer, B. Kramer, and A. MacKinnon, The conductivity of a two-dimensional electronic system of finite width in the presence of a strong perpendicular magnetic field and a random potential, Z. Phys. B **59**, 379 (1985).
[43] Although an in-plane magnetic field can not only reduce the out-of-plane component of the magnetization, but also increase the in-plane component of it, the surface gap is only determined by the out-of-plane component of the magnetization and is unaffected by the in-plane component. Therefore, the decrease in M_z is equivalent to the increase in E_F/M_z.
[44] D. Zhang, M. Shi, T. Zhu, D. Xing, H. Zhang, and J. Wang, Topological Axion States in the Magnetic Insulator $MnBi_2Te_4$ with the Quantized Magnetoelectric Effect, Phys. Rev. Lett. **122**, 206401 (2019).
[45] R. Chen, S. Li, H.-P. Sun, Y. Zhao, H.-Z. Lu, and X. C. Xie, Using nonlocal surface transport to identify the axion insulator, arXiv:2005.14074.
[46] Z.-D. Song, B. Lian, R. Queiroz, R. Ilan, B. A. Bernevig, and A. Stern, Delocalization transition of disordered axion insulator, arXiv:2010.13796.